Termination effects at metal/ceramic junctions: Schottky barrier heights and interface properties of the β-SiC(001)/Ni systems

G. Profeta, A. Blasetti, S. Picozzi, and A. Continenza
Istituto Nazionale di Fisica della Materia (INFM), Dipartimento Fisica, Universitá degli Studi dell'Aquila, 67010 Coppito (L'Aquila), Italy

A. J. Freeman
Department of Physics and Astronomy and Materials Research Center, Northwestern University, Evanston, Illinois 60208
(Received 6 June 2001; published 16 November 2001)

First-principles full-potential linearized augmented plane wave calculations for the β-SiC[001]/Ni interface are presented, focused on the effects of different terminations on the structural and electronic properties. We find a strong reactivity of the interface, as confirmed by the high adhesion energies that are larger for the C-terminated junction than for the Si-terminated junction, in agreement with that previously found for Ti and Al. The metal-induced gap states are efficiently screened in both terminations, resulting in a decay length of about 1 Å. The calculated dependence of the Schottky barrier height on different terminations is not very strong and we investigate the observed differences between Si- and C-terminated junctions in terms of Born effective charges, electronegativity arguments, interface geometries, and screening effects. The agreement with available experimental data is excellent, thus confirming the strong rectifying behavior of this metal/ceramic contact.

DOI: 10.1103/PhysRevB.64.235312 PACS number(s): 73.30.+y, 73.20.At, 73.40.−c

I. INTRODUCTION

In the last few years, SiC has received great attention, both from the experimental and theoretical point of view. This interest is motivated by important physical properties that make SiC well suited for high-power, high-temperature, and high frequency device technology.[1] One of the crucial aspects for device applications is the formation of good metal/SiC contacts, which has motivated the large number of experiments recently performed on this metal/ceramic interface.[2] Among the metals studied, Ni seems to have the highest temperature contacts so that it seems to be the most appropriate metal for high-temperature applications. Indeed, it has been reported that the SiC/Ni interface is stable for temperatures up to 600 °C. Due to the high breakdown electric field and wide-band-gap, high-voltage ($>$200 V) SiC-based Schottky diodes with relatively low leakage current have been fabricated.[3] Ni seems to be a good candidate for this latter application due to the high *n*-type Schottky barrier height ($>$1.2 eV) observed at SiC/Ni contacts. This would allow diode operation at high temperature with lower power losses compared to other metals (e.g., Ti) that have smaller barrier heights.

Stimulated by this growing interest, we present a theoretical first-principles FLAPW (full-potential linearized augmented plane wave) study of the SiC/Ni junction that is, to the best of our knowledge, the first one for this system in both Si (Si-*t*) and C (C-*t*) terminations. In a previous paper,[4] we focused on Ni monolayer adsorption on the SiC surface and analyzed in detail the different possible adsorption sites, the adsorption energies, and the bonding character as a function of both adsorption site and substrate termination. This previous study revealed that the SiC surface is highly reactive for Ni adsorption so that it could succeed in stabilizing the metal growth. In the present paper, we study the Ni/SiC junction, concentrating on the properties that better characterize the interface: heat of formation, Schottky barrier heights (SBH), metal-induced gap states (MIGS), Born effective charges, and core level shifts.

II. TECHNICAL DETAILS

The calculations were performed using the all-electron FLAPW method[5] within density functional theory in the local density approximation. In the basis set, wave functions with wave vector up to $k_{max}=4.2$ a.u. were included, leading to about 2000 basis functions; an angular momentum expansion up to $l_{max}=8$ was used for the potential and the charge density representations. The Brillouin zone sampling was performed using 20 special *k* points according to the Monkhorst-Pack scheme.[6] The muffin-tin radii R_{MT} used for Si, C, and Ni were 2.1, 1.4, and 2.0 a.u., respectively. The supercell considered contains 11 SiC layers and 7 Ni layers (11+7); tests on the cell dimension show that bulk conditions are well recovered away from the interface (the Schottky barrier height is stable to within 0.01 eV if supercell dimensions are increased up to 19+9 layers).

III. STRUCTURAL PROPERTIES

We deal with both the Si-terminated and C-terminated SiC/Ni interfaces. The calculated bulk lattice constants of the cubic SiC (3C-SiC) and paramagnetic fcc Ni are 4.34 Å and 3.43 Å, respectively. We calculated the most stable interface geometries, assuming pseudomorphic growth conditions along the [001] direction. To reduce the very large mismatch at the interface ($\sim$27%), we rotate the Ni overlayer by 45° with respect to SiC ($a_{overlayer}=a_{SiC}/\sqrt{2}$). However, the mismatch is still quite large (of the order of 10%). The supercell contains one atom per layer in the SiC region and two atoms per layer in the Ni region. At the interface, the two Ni

TABLE I. Structural data in angstrom.

	Si term	C term
Interface bond length	2.24 (d_{Si-Ni_b})	1.92 (d_{C-Ni_b})
Interface bond length	+1% (d_{Si-C})	Bulk (d_{C-Si})
Vertical buckling	0.55	0.23
Ni interplanar distance	1.93	1.93

atoms occupy the bridge (Ni_b) and antibridge (Ni_a) adsorption sites, as conventionally labeled. The two sites differ in their coordinations with respect to the substrate atoms: while the bridge site corresponds exactly to a zinc-blende site, the antibridge position is an empty site of the zinc-blende lattice and lays on top of the sub-surface layer sites. As a consequence, the atom at the bridge site points towards the *s-p* hybrids of the substrate atoms, while the one on the antibridge site will have no tetrahedral bonds to coordinate with.

The Ni-Ni interplanar distance in the bulk region was optimized by performing a tetragonal distortion of bulk fcc Ni along the growth direction and keeping the in-plane lattice constant constrained to bulk SiC. The calculated value, $d_{Ni\text{-}Ni}=1.93$ Å, is in excellent agreement with the macroscopic theory of elasticity[7] predictions ($d^{MTE}_{Ni-Ni}=1.92$ Å). All the free structural parameters in the supercell are then optimized according to the Hellmann-Feymann forces. The resulting structural data for the equilibrium geometry are reported in Table I. The two Ni sites are no longer on the same horizontal plane but show a vertical buckling: in fact, the Ni atom occupying the bridge site is in line with the semiconductor sp^3 dangling bonds, and therefore shows stronger hybridization and shorter bond length (see discussion below). The Ni in the antibridge site, on the other hand, moves away from its ideal position. The buckling effect is mainly localized at the interface: the bulk conditions are already recovered starting from the second Ni layer. The main difference between the two SiC terminations is due to size effects: the Si-Ni bond length is larger than the C-Ni bond length (by 0.32 Å), in excellent agreement with the difference between Si and C covalent radii (0.33 Å). As regards the SiC substrate relaxation, we find only a small deviation from the SiC bulk bond length only in the Si-*t* case for the subsurface bonds.

IV. ADHESION ENERGY

We recall that the adhesion energy (E_{adh}) is defined as the energy gain per unit area due to interface formation, taking as reference the two relaxed (1×1) surfaces, with area *A*. This can be calculated subtracting from the total energy of the supercell (E_{sup}) that of the relaxed (and tetragonally strained in the Ni case) clean constituent surfaces (E_{SiC} and E_{Ni}).

$$E_{adh}=\frac{1}{2A}(E_{sup}-E_{SiC}-E_{Ni}),$$

TABLE II. Adhesion energy (J/m^2) for the SiC(001)/Ni interface. Results for the SiC(001)/Ti and SiC(001)/Al interfaces are taken from Refs. 8 and 9

	Si term	C term
SiC(001)/Ni interface	6.21	8.63
SiC(001)/Ti interface	2.52	8.74
SiC(001)/Al interface	3.74	6.42

where the factor 2 takes into account the two identical interfaces in the supercell. The calculated adhesion energies are shown in Table II, where other available theoretical data for SiC/Al and SiC/Ti interfaces[8,9] are reported for comparison. Our FLAPW calculations show that there is a large energy gain in the formation of the SiC/Ni interface. For the Si-*t* interface, this energy is the largest reported in Table II; this indicates the strong reactivity of the SiC/Ni interface and possible strong Si-Ni and C-Ni bonding formation (see discussion below). In the nonreactive case (e.g., MgO/Al), in fact, adhesion energies are much smaller ($1.1\ J\,m^{-2}$).[10] However, in the case of SiC/Al and SiC/Ti, the unit cell contains only one Ti or Al atom per layer, still assuming a (1×1) in-plane periodicity. This choice is induced by strain considerations, since both Ti and Al have large lattice constants that match the SiC substrate much better than Ni.

In order to gain insights into these large adhesion energy values, it is useful to separate chemical from structural effects; we therefore let the Ni overlayer expand, in order to recover the same geometry as in the Ti and Al case, having one atom per layer. This system itself (referred to as 1Ni/SiC) is quite unrealistic since too large an Ni in-plane expansion (up to 27%) is required. The most energetically favorable position of the interface Ni atom is the bridge site for both terminations and we again relax all the internal parameters. For the Si-*t* interface, we find an equilibrium Si-Ni

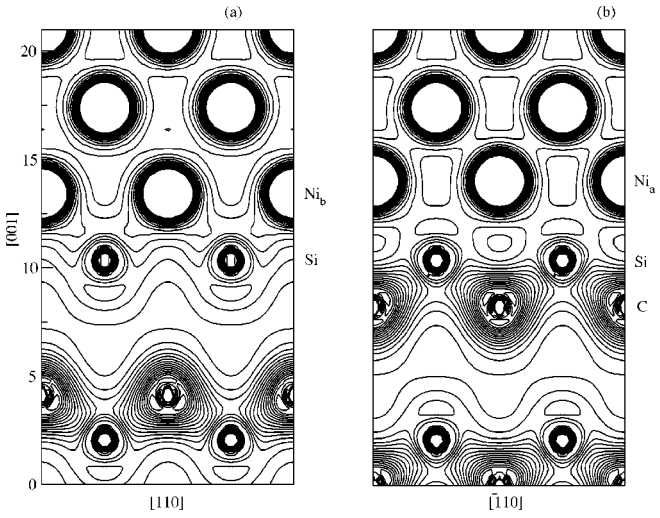

FIG. 1. Valence charge density for the Si-terminated SiC(001)/Ni interface. Contours are plotted from 0.007 to 1.9 with a spacing of 0.1 in e Å^{-3}.

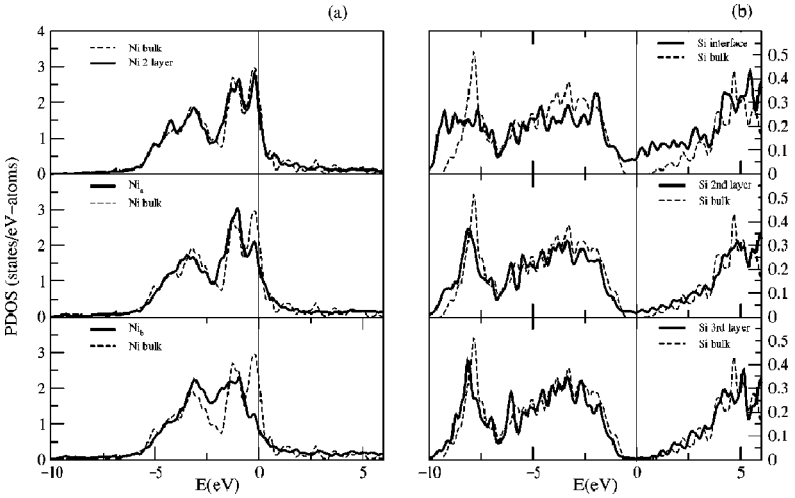

FIG. 2. PDOS for the Si-terminated SiC(001)/Ni interface. The dashed line represents the bulk value and the vertical line denotes the Fermi level (zero of the energy scale).

interlayer distance of 1.65 Å, while for C-*t* the equilibrium C-Ni distance is 0.93 Å. These values have to be compared with the interlayer spacing between the Ni_b and the substrate, found previously; namely, 1.63 and 1.15 Å for Si-*t* and C-*t*, respectively. The calculated adhesion energies are now 5.8 and 8.8 J/m^2, for the Si-*t* and C-*t*, respectively. These results confirm the reactivity of the surface, related to a strong chemical bond formation between Ni and Si (C) atoms. From the data of both structures (1Ni/SiC and 2Ni/SiC), a trend emerges: the C-*t* adhesion energy is always larger than the Si-*t* one. Moreover, based on strain considerations, it is expected that in real conditions there will be more than one Ni surface adatom per (1×1) SiC unit-cell, thus confirming our unit cell choice.

V. ELECTRONIC PROPERTIES

In order to give a rationale for the strong adhesion energy values observed and to understand the nature of the bonding formation at the interface, we investigate the electronic properties of the interface in terms of charge density distribution, core levels, and density of states.

A. The Si-terminated interface

Figure 1 shows the Si-*t* valence charge density distribution on two vertical planes cutting the interface Si-Ni_b bond (left panel) and the interface Si-Ni_a (right panel) bond, respectively. On the (110) plane [Fig. 1(a)], we can see that the spherical symmetry in the metal side is broken at the Ni occupying the bridge site: two bonding humps are directed towards the neighboring Si atoms. Quite different features are observed for the charge on the $[\bar{1}10]$ plane [Fig. 1(b)]. No evident bonding features between Ni and Si are observed. As expected, the Si-Ni interaction is stronger for Ni in the bridge adsorption site than in the antibridge site. Figure 2 shows the site-projected partial density of states (PDOS) for the Si-*t* interface. From inspection of the DOS, we find that bulk conditions are well recovered already in the second metal layer and that the high DOS at the Fermi level (E_F), characteristic of bulk Ni, decreases in moving towards the interface.

As already noted from the charge density plot, Ni_a and Ni_b have quite different features: inspection of the PDOS reveals that the contribution to Si-Ni hybridization is more pronounced for Ni_b. Also, comparing with the PDOS in bulk Ni (dashed lines in Fig. 2), we find that on Ni_b some states move away from E_F towards higher binding energies. As far as Ni_a is concerned, only states in a small region close to E_F differ substantially from the bulk. The right panel in Fig. 2 shows the DOS projected on the interface Si site and on the two subsurface Si layers (2nd and 3rd). Bulk conditions are perfectly recovered in the inner layer (3rd layer) showing that the supercell dimensions are large enough for our purposes. The DOS projected on interface Si atom clearly reveals the presence of MIGS in the band-gap region. We notice a deviation from the bulk behavior in the *p* band between -4.5 and 2.5 eV and in the *s* band between -7.5 and -10 eV; this suggests that the orbitals involved in the bonding are Si-*sp* and Ni-*d*. The MIGS decrease rapidly in the semiconductor region and completely disappear on the inner Si layer.

Further insights into the nature of the gap states can be gained from their spatial localization. We plot in Figs. 3(a) and 3(b) the charge density due to the occupied MIGS, on the [110] and $[\bar{1}10]$ planes. These states are mainly localized in the interface region with a resonant behavior in the Ni side and a negligible dispersion in the SiC region. Performing a planar macroscopic average,[11] as shown in Fig. 3(c), and assuming an exponential decay in the semiconductor side, we can estimate the decay length for the MIGS: $\lambda_{SiC}\sim1$ Å. The MIGS tend to vanish very quickly in the SiC side and determine a metallic behavior very localized at the interface with a decay length smaller than that of other semiconductors such as GaAs (Refs. 12 and 13) ($\lambda_{GaAs}\sim3$ Å) and GaN (Ref. 14) ($\lambda_{GaN}\sim2$ Å).

The interface effects on the charge rearrangement can be investigated in a more quantitative way by analyzing the core level shifts (Si 1*s* and Ni 1*s*) and the variation of the MT charge with respect to the bulk value as a function of the distance from the interface (not shown). The Ni and Si core levels bend (by about 0.2 eV) on going from bulk towards the interface region and follow the same trend (i.e., the bind-

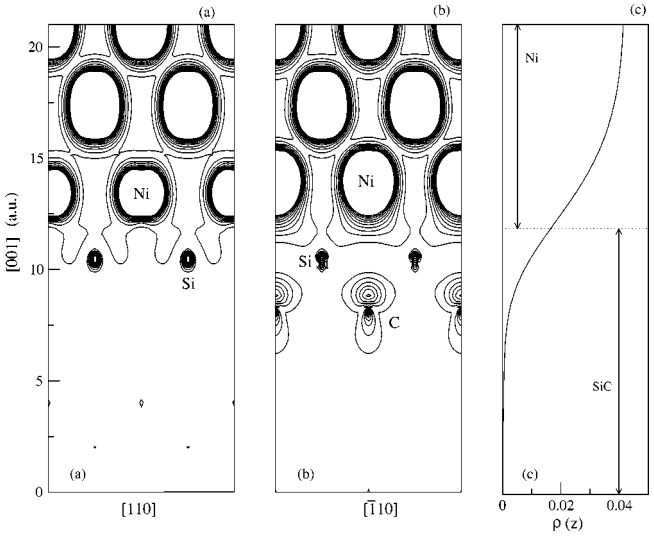

FIG. 3. Charge density for the MIGS states [Figs. 3(a), (b)]. Contours are plotted from 0.007 to 0.07, spaced by 0.007 e Å^{-3}) and macroscopic average of the MIGS charge density [Fig. (3c)].

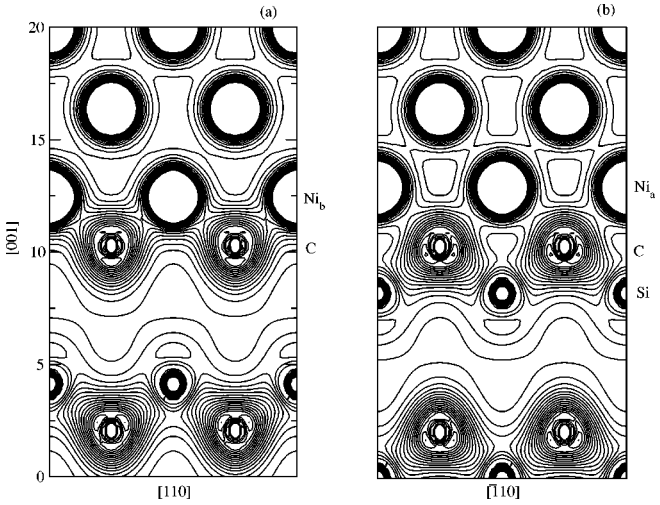

FIG. 4. Valence charge density for the C-terminated SiC(001)/Ni interface. Isocharge contour from 0.007 to 1.8 spaced by 0.1 e Å^{-3}).

ing energy is larger at the interface than in the inner layer). The core level shifts are consistent with the observed charge transfer, if we subtract out the Madelung contribution[15] from the core level binding energies. The present results are consistent with those found previously[4] for the monolayer Ni and are therefore not shown.

B. The C-terminated interface

Figure 4 shows the valence charge distribution for the C-t SiC/Ni interface on the same planes used for the Si-t (cf. Fig. 1). The strong bonding nature of this termination is evident from the rather large charge density present at the interface between Ni and C. In particular, we find non-negligible charge on the C-Ni$_b$ bond. This is consistent with the large adhesion energy associated with this termination. As already observed for the Si-t interface, Ni in the antibridge adsorption site shows a weaker bond.

We report in Fig. 5 the PDOS for the C-t: Fig. 5(a) shows the DOS projected on the two interface Ni and on the subsurface Ni with respect to the bulk (dashed line). No remarkable differences appear with respect to the Si-t interface. The DOS at the interface C and at the two subsurface C atoms are plotted in Fig. 5(b) and compared with the bulk PDOS. The features on the interface C atom are very clear: in the energy region between -10 eV and -1 eV, the character is mainly p type while s states, due to their higher binding energy, do not participate in the hybridization. The overall shape of the interface C PDOS shows a depletion of states in the region from -4 eV to the valence-band maximum (VBM). These states hybridize with Ni $3d$ states and show bonding/antibonding features. The bonding part is located around -5 eV, where new states appear with respect to the bulk. The antibonding partners are pushed to higher energies, from VBM up to 2 eV: these states give rise to the MIGS. It is important to note, in the region close to E_F, that the DOS is higher than in the Si-t, probably due to the presence of the antibonding contribution just mentioned. As we will discuss later, this is responsible for the different screening properties found in Si-t and C-t.

The MIGS charge density contour plots are formally identical to the Si-t interface and are, therefore, not shown; the calculated MIGS decay length is found to be equal to the Si-t case, confirming that the decay length is a semiconductor bulk property and thus is termination independent.

VI. SCHOTTKY BARRIER HEIGHTS

The SBH is calculated adopting the usual procedure[16,17] that takes core levels as reference energies. We express the barrier height as the sum of two terms:

$$\Phi_B = \Delta b + \Delta E_b \tag{1}$$

Δb and ΔE_b denote an *interface* and a *bulk* contribution, respectively. As reference core levels, we take the $1s$ level both for Ni and Si (or C): $\Delta b = E_{1s}^{Si(C)} - E_{1s}^{Ni}$. A stability of a few hundredths of eV of the barrier heights was observed for a different choice of the reference core levels, leading to a total uncertainty of 0.05 eV in the final SBH. The *bulk* contribution can be evaluated from separate calculations of bulk SiC and strained Ni and the difference between the binding energies of the same $1s$ levels considered above: $\Delta E_b = (E_{VBM}^{SiC} - E_{1s}^{Si(C)}) - (E_F^{Ni} - E_{1s}^{Ni})$. The p-type SBH values obtained are shown in Table III and compared with calculations for Al and Ti junctions.[8,9] The values for the SiC/Ni interface calculated from the core levels are in good agreement with those evaluated from the density of states, defining Φ_B as the energy difference between E_F and the VBM of the inner semiconductor layer (within 0.1–0.2 eV); note that this last procedure introduces errors due to the nonperfect determination of the VBM. If we evaluate the n-type SBH by using the experimental band gap, we find for the Si-t interface a SBH of 1.40 eV, in good agreement with the value estimated for the 4H-SiC/Ni interface (1.3 eV).[18]

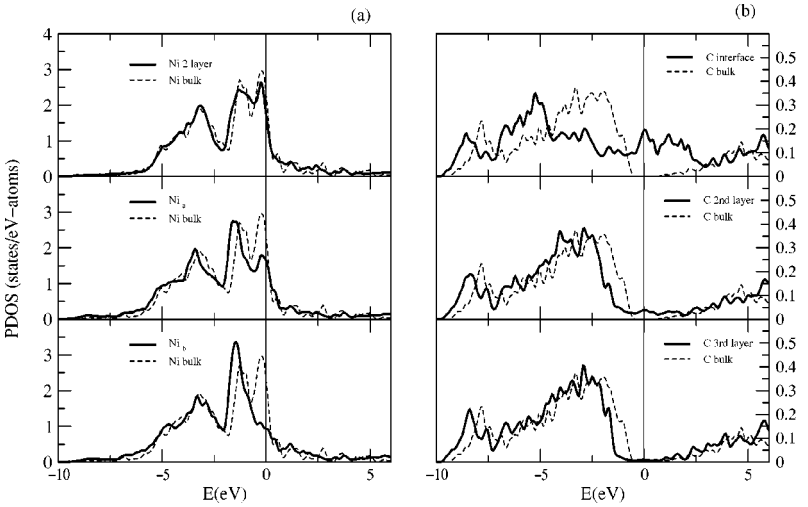

FIG. 5. PDOS for the C-terminated SiC(001)/Ni interface. The dashed line represents the bulk value, the vertical line represents the Fermi level (zero of the energy scale).

The *p*-type SBH for the Si-*t* interface is smaller than that for the C-*t* interface (by about 0.3 eV). The theoretical SBH values for Ti and Al (the only ones found in the literature for SiC) can be understood on the basis of the results obtained for Ni/SiC. Being a transition metal (TM) with *d* orbitals participating in the bond, Ti can be directly compared with Ni. In both cases, we find the same difference (i.e., 0.3 eV in absolute value) between the SBH at the two terminations, but the trend with the termination is opposite and the absolute values of the Ti SBH's are smaller than in Ni. The first observation can be justified in a qualitative way, recalling that Ti has two electrons in the *d* shell, while Ni has two ''holes,'' thus suggesting somehow opposite chemical properties. It is therefore reasonable to expect a reversed charge transfer at the interface[19] leading to an opposite interface dipole orientation and to a consequently reversed trend as a function of the SiC termination. Moreover, the Schottky model[20] gives SBH linearly dependent on the metal work function ϕ_M ($\phi_{Ti}=4.3$ eV and $\phi_{Ni}=5.22$ eV), confirming the observed trend between the two metals.

The comparison with Al is more complicated due to the very different nature of the chemical bonds at the interface between a TM and a free-electron metal such as Al.[21] Moreover, we observe that, at variance with Ti and Ni, the SBH variation with the SiC termination is appreciable (about 0.8 eV). The response of the metal to the two Si- and C-semiconductor terminations (which, as we showed, are remarkably different) is mainly governed by the DOS at E_F. This is quite high for TM, due to localized *d* states producing high DOS localized around E_F that are essentially able to pin the Fermi level in a relatively small region independent of SiC termination. On the other hand, the DOS at E_F is smaller for Al, which indeed shows a larger variation of the SBH with the SiC termination.

TABLE III. Calculated *p*-type SBH (eV) for the C-terminated and Si-terminated SiC/Ni interface. Results for SiC/Al and SiC/Ti from Refs. 8 and 9 are also listed.

	Si term	C term
SiC(001)/Ni	0.90	1.19
SiC(001)/Ti	0.50	0.22
SiC(001)/Al	0.85	0.08

In addition to chemical effects related to the metal species, the SBH is strongly dependent on the interface structural geometry that, in principle, can even reverse the observed trend with respect to the semiconductor (ceramic) termination. As stated before, the unit cell adopted in the present study contains two Ni atoms per layer on the metal side (2Ni/1SiC), while previous studies[8,9] with Al and Ti were performed with one atom per layer. In order to understand possible structural effects on the SBH formation, we calculated the SBH variations due to strain on the metal, thus considering the case of one Ni atom per in-plane unit cell (1Ni/1SiC). The calculated SBH is in this case 0.70 eV for the Si-*t* case and 1.0 eV for the C-*t*. These values follow exactly the same trend observed in the previous geometry, even if the absolute values are now smaller (by about 0.2 eV). It is very interesting to investigate these differences further. First, we note that the SBH [see Eq. (1)] accounts for a bulk contribution (ΔE_b) that comes from the relative position of the metal Fermi level and the semiconductor VBM of the isolated bulk materials. This term varies with the strain conditions: actually, we find that the core-level binding energy variation in bulk Ni is equal to 0.1 eV. Therefore, since the total SBH variation is about 0.2 eV, we can infer that the remaining 0.1 eV has to be ascribed to contributions coming from the interface term (Δb).

In addition, we note that while in the Si-*t* case the interplanar distance between the substrate and the metal is quite insensitive to strain conditions (from 1.65 to 1.63 Å), in the C-*t* case there is a compression of about 20% (see discussion in Sec. III). Nevertheless, the relative variation of the SBH is the same for both terminations. Now, the SBH variation due to bond-length relaxation can be explained if we evaluate the longitudinal interface effective charge[22] Z_L^* in the 2Ni/1SiC case in both terminations. For Si-*t* we find $Z_L^*(\mathrm{Si})=+0.08$ and $Z_L^*(\mathrm{Ni})=-0.04$, while for C-*t*: $Z_L^*(\mathrm{C})=-0.08$ and $Z_L^*(\mathrm{Ni})=+0.007$. Therefore, in the Si-*t* case, $Z_L^*(\mathrm{Ni})$ is nearly an order of magnitude greater than the $Z_L^*(\mathrm{Ni})$ in the

C term. If we calculate the same quantities in the 1 Ni/1SiC case, we find the same trend, but with absolute values that are about four times larger. These results demonstrate two different and relevant aspects that characterize the different terminations. (i) The C-*t* interface has a stronger metallic character: this is confirmed by the effective charges and PDOS on the interface C atom (see Fig 5), showing a higher DOS at E_F with respect to the Si-*t* case (the same is found in the 1 Ni/1SiC case, not shown). In fact, if we take the equilibrium Si-*t* interface and exchange C and Si, we obtain a C-*t* interface with distances that are about +43% larger (0.48 Å) than its own equilibrium: the SBH changes only by 0.1 eV. (ii) The values of Z_L^*(Ni) are also dependent on the intrinsic Ni metallicity. Z_L^*(Ni) increases on going from 2 Ni to 1 Ni, due to the unphysical large strain condition of 1Ni/1SiC and to the lower DOS at E_F contributed by only one Ni per cell. Moreover, let us consider the 1Ni/1SiC case and bring the Ni-substrate distance from 1.77 to 1.153 Å (i.e., we force the Ni to occupy the Ni_b position in the case of 2Ni/1SiC in the C-*t*). This increases the Ni-substrate distance by about 20% and leads to a SBH variation of −0.2 eV. The SBH variation is, therefore, larger than that discussed in (i) for an overall much smaller structural change, therefore indicating a loss of metallicity and an increased Z_L^*(Ni) in going from 2Ni/1SiC to 1Ni/SiC.

At this point, we can draw some conclusions concerning the SBH: the values calculated for both 2Ni and 1Ni interface structures are consistent with trends found as a function of the metal and semiconductor terminations. We were able to separate bulk and interface contributions to the SBH due to different strain conditions. In particular, we found that the different metallic interface configurations considered contribute 0.1 eV to the bulk-term and 0.1 eV to the interface term, for both terminations. Independent of the interface geometry, the effective charge on the interface metal atom in the C-*t* shows a more metallic behavior with respect to the Si-*t*: this is related to the different screening properties, associated with the MIGS and more in detail on the charge redistribution on the interface atom.

VII. CONCLUSIONS

We have carried out an *ab initio* study of the β-SiC(001)/Ni interface, focusing on the effects of the different termination and comparing our results with those obtained for other metal/SiC interfaces (available in the literature). The high adhesion energies found confirm the strong reactivity of the interface, and are shown to be related to the remarkable *p*-*d* hybridization between the substrate atom and the Ni at the bridge site. We also showed that the strong bond between the substrate and the Ni at bridge site makes the adhesion energy quite independent on strain conditions. The values of the calculated SBH lead to the conclusion that the ideal metal-semiconductor contact is rectifying. In addition, we find that the SBH value of the two different terminations are sensitive (within 0.2 eV) to strain modifications and interfacial geometry changes. This suggests that the high density of MIGS, originating from *p*-*d* hybridization, is able to pin the Fermi level in quite a small region within the semiconductor band gap.

ACKNOWLEDGMENTS

We acknowledge support by an INFM supercomputing grant at Cineca (Bologna, Italy) through *Progetto Calcolo Parallelo*. Work at Northwestern University was supported by the U.S. Department of Energy (under Grant No. DE-F602-88ER45372).

[1] *SiC Materials and Devices, Vol. 52 of Semiconductors and Semimetals*, edited by Y. S. Park (Academic Press, San Diego, 1998).
[2] R. Kaplan and V. M. Bermudez, in *Properties of Silicon Carbide*, EMIS Data reviews Series, No. 13, edited by G. L. Harris (INSPEC, London, 1995) p. 101.
[3] V. Saxena, J. N. Su, and A. J. Steckl, IEEE Trans. Electron Devices **46**, 456 (1999).
[4] G. Profeta, A. Continenza, and A. J. Freeman, Phys. Rev. B **64**, 045303 (2001).
[5] H. J. F. Jansen and A. J. Freeman, Phys. Rev. B **30**, 561 (1984); M. Weinert, H. Krakauer, E. Wimmer, and A. J. Freeman, *ibid.* **24**, 864 (1981), and reference therein.
[6] H. J. Monkhorst and J. D. Park, Phys. Rev. B **13**, 5188 (1976).
[7] C. G. Van de Walle, Phys. Rev. B **39**, 1871 (1988).
[8] M. Kohyama and J. Hoekstra, Phys. Rev. B **61**, 2672 (2000).
[9] J. Hoekstra and M. Kohyama, Phys. Rev. B **57**, 2334 (1998).
[10] J. R. Smith, Tao Hong, and D. J. Drolovitz, Phys. Rev. Lett. **72**, 4021 (1994).
[11] A. Baldereschi, S. Baroni, and R. Resta, Phys. Rev. Lett. **61**, 734 (1988).
[12] S. G. Louie, J. R. Chelikowsky, and M. L. Cohen, Phys. Rev. B **15**, 2154 (1977).
[13] C. Berthod, J. Bardi, N. Binggeli, and A. Baldereschi, J. Vac. Sci. Technol. B **14**, 3000 (1996); M. Peressi, N. Binggeli, and A. Baldereschi, J. Phys. D **31**, 1273 (1998).
[14] S. Picozzi, A. Continenza, G. Satta, S. Massidda, and A. J. Freeman, Phys. Rev. B **61**, 16 736 (2000).
[15] S. Ossicini, C. Arcangeli, and O. Bisi, Phys. Rev. B **43**, 9823 (1991).
[16] S. H. Wei and A. Zunger, Phys. Rev. Lett. **59**, 144 (1987).
[17] S. Massidda, B. I. Min, and A. J. Freeman, Phys. Rev. B **35**, 9871 (1987).
[18] K. J. Schoen, J. M. Woodall, and J. A. Cooper, IEEE Trans. Electron Devices **45**, 1595 (1998).
[19] S. R. Nishitani, S. Fujii, M. Mizuno, I. Tanaka, and H. Adachi, Phys. Rev. B **58**, 9741 (1998).
[20] W. Schottky, Phys. Z. **41**, 570 (1940).
[21] M. van Schilfgaarde and N. Newman, Phys. Rev. Lett. **65**, 2728 (1990).
[22] A. Ruini, R. Resta, and S. Baroni, Phys. Rev. B **57**, 5742 (1998).